IEEE Access
Multidisciplinary | Rapid Review | Open Access Journal

Received April 9, 2020, accepted April 23, 2020, date of publication May 6, 2020, date of current version May 20, 2020.

Digital Object Identifier 10.1109/ACCESS.2020.2992466

UAV-Aided Wireless Communication Design With Energy Constraint in Space-Air-Ground Integrated Green IoT Networks

HAIBO DAI[1,2], (Member, IEEE), HUI BIAN[2], CHUNGUO LI[2], (Senior Member, IEEE), AND BAOYUN WANG[3], (Member, IEEE)

[1]School of Internet of Things, Nanjing University of Posts and Telecommunications, Nanjing 210003, China
[2]School of Information Science and Engineering, Southeast University, Nanjing 210096, China
[3]School of Communication and Information Engineering, Nanjing University of Posts and Telecommunications, Nanjing 210003, China

Corresponding author: Haibo Dai (hbdai@njupt.edu.cn)

This work was supported in part by the Natural Science Foundation of China under Grant 61801243, Grant 61671144, Grant 61971235, and Grant 61971238, in part by the China Postdoctoral Science Foundation under Grant 2019M651914, in part by the Natural Science Foundation of the Jiangsu Higher Education Institutions of China under Grant 18KJB510026, and in part by the Foundation of Nanjing University of Posts and Telecommunications under Grant NY218124.

ABSTRACT As more vehicles connect to the internet, they become an important and growing segment of Internet of Things (IoT). To enhance the performance of vehicle-to-network (V2N) communication with green objectives, satellite and unmanned aerial vehicle (UAV) are jointly applied to aid ground communication facility by leveraging the coordinated multi-point transmission technique. This paper investigates a novel architecture of V2N communication in the space-air-ground integrated IoT network consisted of ground base stations (BSs), a UAV as well as one satellite. In the V2N communication model, the UAV, receiving the requested data from the satellite, and BS cooperatively serve the ground vehicle. The goal of this paper is to maximize the achievable rate of the ground vehicle by jointly optimizing the transmit power allocations (i.e., UAV and ground BS) and UAV trajectory, subjecting to the UAV energy constraint, UAV transmission constraint as well as UAV mobility constraint. However, there exists an intractable issue of the formulated problem in a complicated non-convex form. To this end, we decompose it into two sub-problems by fixing UAV trajectory and the power allocations alternately. Specifically, the closed-form expressions are derived to solve the sub-problem with the given UAV trajectory. For the sub-problem with the given power allocations, the UAV trajectory is calculated by using successive convex approximation (SCA) technique. Through the alternation of two methods and iterative operation, the joint optimal solution to the problem is achieved. Finally, numerical results verify that UAV plays a pivotal role in overcoming the tradeoff between higher performance and green communication.

INDEX TERMS Space-air-ground integrated green IoT networks, energy constraint, vehicle-to-network, coordinated multi-point transmission, UAV trajectory optimization.

I. INTRODUCTION

Internet of Things (IoT) is rapidly changing how we live [1]–[4]. This is particularly true of the field of intelligent transportation, which is where some of the biggest innovations are being developed and implemented [5], [6]. Machina research shows that the connected vehicle market is one of the highest growth areas of the IoT, with a potential application revenue of $USD 253 billion by 2025. In recent years, vehicle-to-network (V2N) communication has attracted considerable attention for the purposes of high reliability of data transmission and intelligent driving [7]–[10]. According to the report of the relevant research institution (i.e., IHS Markit), the sales volume of car communications products is predicted to reach 5.6 million sets by the year 2020 and then broke through 55 million sets by the year 2025. It is urgent to build a robust communication facility for supporting the various demands from V2N communications [11]–[13].

The associate editor coordinating the review of this manuscript and approving it for publication was Jun Wu.

A conventional method is to deploy a sequence of ground base stations (BSs) at the roadside, as the network access point of the ground vehicles [14]. When the interval between two adjacent BSs is relatively large, the mobility of the vehicle gives rise to great challenge to guarantee both the stability of the communication link and the full coverage [15], [16]. Conversely, the dense deployment of BSs brings the considerable stress of deployment costs to the communication operator and the problem of frequent handover caused by the vehicles' movement [17]. Moreover, the character of tidal transportation results in the challenge to find the optimal tradeoff between communication performance and economic efficiency in V2N communication architecture [18], [19].

To achieve high throughput and high reliability data delivery, satellite networks and UAV systems in space or air are exploited [20]–[23]. The reason for not only depending on the ground communication systems is that it cannot be guaranteed to provide wireless access services with high data rate and reliability at any place of the highway system [24]. Therefore, with the help of the UAV communication platform and satellite systems, a new network architecture is exploited to accommodate diverse services and applications with different quality of service requirements in V2N communication scenario [25]. The new network architecture is the integration of space-air-ground network segments [26]. The vehicle gets access to it by the cooperation of UAV and the ground BS. The UAV, as an air communication platform, can be flexibly deployed or withdrawn to assist the ground BSs according to the flow of traffic. Moreover, the UAV plays a role of relay to transmit the information received from the satellite to the vehicle. It is undeniable that the new architecture of communication system faces some challenges. The optimization of UAV trajectory and power control has important impact on the performances for information exchanging.

Next, we give a brief review of the works related to our research. More related works on the efficient V2N communication can be found in [27]–[31]. To guarantee the latency and reliability requirements of vehicles while maximizing the information rates of cellular users, Mei *et al.* in [27] proposed jointly optimizing the radio resource, power allocation, and modulation/coding schemes of the vehicle-to-vehicle (V2V) communications. By using deep reinforcement learning, [28] proposed a decentralized resource allocation mechanism for the V2V communications. The decentralized method does not require the global information exchange and has the small transmission overhead. Since vehicle-to-infrastructure (V2I) communications in a multi-vehicle environment highly depend on the accurate channel estimation, Xu *et al.* in [29] proposed an effective channel training protocol. The resource allocation problem is investigated in device-to-device-based vehicular communications [30]. [31] used stochastic geometry to analyze the coverage of urban millimeter-wave cellular networks, which is used as the infrastructure for V2I communications.

Due to the inherent advantages in terms of large coverage, mobility and flexibility, the satellite-terrestrial network and the UAV-assisted communication system have attracted much attention and research [32], [33]. [32] studied the energy-efficient optimization problem in the satellite-terrestrial spectrum sharing scheme. To enhance the security of the satellite link, Li *et al.* in [33] was to optimize the joint cooperative beamforming and artificial noise under constraints of the secrecy rate constraint and the information rate. On the other hand, the coexistence problem of both the satellite and the ground BS is studied [34]–[36]. The secure beamforming issue was investigated in [34] to ensure 5G cellular system coexisting with a satellite network. Since the seamless coverage supporting by the cooperation of the satellite and ground BSs, Zhang *et al.* in [35] investigated the problem of joint user access and resource allocation in the cooperative multicast satellite-terrestrial network. Similarly, a novel cooperative transmission strategy was proposed to be used in the cognitive satellite networks, where BS or mobile users in the cellular network helps the communication of the satellite network [36]. The UAV is used to aid the ground BS to serve users [37]–[39]. Under situation of guaranteeing the interference temperature constraint on the satellite network, the UAV and BS adopted joint transmission to enhance the terrestrial network performance in [37]. By improving energy-efficiency, multiple UAVs were deployed to make the coverage scenario more reliable and efficient [38]. To improve the throughput and delay performance, Joo *et al.* in [39] proposed a relay architecture with UAV between the ground and satellites to facilitate satellite access with a low overhead.

II. METHODOLOGY

Bearing the above in mind, we tend to leverage Lagrange method and successive convex approximation (SCA) technique to solve the joint UAV trajectory and power control problem for green V2N communication in space-air-ground integrated IoT network. In this paper, we assume that the vehicle gets access to the communication infrastructure with the help of UAV and satellite, and it is looking forward to satisfying the request of the high speed of data transmission for the ground vehicle under UAV's energy constraint. Certainly, this is confronted with more challenges. The V2N communication has the demand of the stable and reliable data transmission. However, both the mobility of the vehicle and the interference from other ground BSs greatly affect the communication quality. The non-convex optimization objective and constraints bring a great challenge to achieve the rational strategies of both power control and UAV trajectory. In this paper, we study the joint UAV trajectory and power optimization problem with energy constraint to achieve the optimal performance of the communication infrastructure in the space-air-ground integrated IoT network. The main contributions to our work are summarized as follows:

- We propose a novel architecture of V2N communication to provide the vehicle with the stable and reliable communication links. Since the vehicle movement causes the instability of the link between the vehicle and the ground

BS, the coordinated multi-point transmission method is applied to our scenario. The UAV, considered as a relay of receiving information from the satellite, and the ground BS cooperatively transmit information to the ground vehicle.

- Considering that the optimization problem is in a multi-variable and non-convex form which is unable to be directly tackled by the existing approaches, we equivalently convert it into two subproblems by fixing UAV trajectory and power alternately. Finally, we develop a two-layer iterative algorithm to solve the optimization problem by using SCA technique.
- For the power control subproblem, we convert it into a convex optimization problem by using the logarithmic approximation method. According to the derived closed-form expressions, a low-complexity algorithm is then proposed to obtain the optimal transmit power strategies of the UAV and the associated BS. For the UAV trajectory subproblem, we propose an efficient algorithm to optimize the UAV trajectory via using the SCA technique.

The rest of this paper is organized as follows. In Section III, the system model and the optimization problem are presented. According to the presented system model, Section IV decomposes the optimization problem into two subproblems by alternately fixing one of two kinds of variables (i.e., UAV trajectory and power control), and then proposes the corresponding algorithms. Finally, numerical results and discussion are presented in Section V, and Section VI concludes this paper.

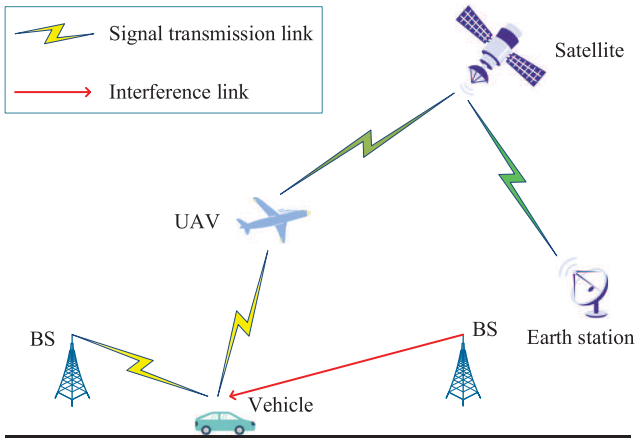

FIGURE 1. An illustrative structure of space-air-ground integrated green IoT networks to serve vehicle-mounted communication terminals.

III. SYSTEM MODEL AND PROBLEM FORMULATION

A. SYSTEM MODEL

We consider an architecture of the satellite-air-ground integrated IoT network illustrated in Fig. 1, which consists of the satellite, UAV and the ground BSs to provide the ground vehicle with improved and flexible end to end service. By the roadside, the ground BSs are deployed at regular intervals. When a vehicle runs on the road, UAV and BS jointly transmit same data to the vehicle. BSs are connected to the content server via optical fiber links while UAV is connected to the content server by the satellite link.

Suppose that the UAV is low-altitude fixed-wing aircraft and can freely adjust its moving direction in a horizontal plane with a fixed altitude during time horizon T. To make the problem more tractable, the flight time T is approximately divided into N time slots and each time slot duration is $\Delta t = \frac{T}{N}$. The location of UAV at time slot n is denoted by $\mathbf{W}[n] = (\mathbf{w}[n], h)$, where $\mathbf{w}[n]$ denotes the horizontal coordinate and h is the flight altitude. The ground vehicle is assumed to keep an even speed for simplicity and the horizontal coordinate at time slot n is $\mathbf{l}_v[n]$. With the purpose of receiving the strongest signal, the ground vehicle is generally associated with the closer BS at time slot n, termed as b_n, and it's location is denoted as $\mathbf{l}_b[n]$. According to the above assumptions that the ground BSs are deployed at regular intervals and the ground vehicle is associated with the closest BS, the vehicle receives the interference signal from the adjacent BS that it is termed as b'_n at time slot n and it's location is denoted as $\mathbf{l}_{b'}[n]$.

Since the carried battery capacity is constrained due to the limited size of UAV, the energy consumption of UAV becomes a huge challenging to the UAV-to-ground communication system. Compared with the communication-related energy consumption, the propulsion-related consumption is dominating during the flight of UAV, which is formulated by

$$\Xi(\mathbf{v}[n], \mathbf{a}[n]) = \sum_{n=1}^{N} \left(c_1 \|\mathbf{v}[n]\|^3 + \frac{c_2}{\|\mathbf{v}[n]\|} \left(1 + \frac{\|\mathbf{a}[n]\|^2}{g^2} \right) \right) + \frac{1}{2} m (\|\mathbf{v}[T]\|^2 - \|\mathbf{v}[0]\|^2), \quad (1)$$

where $c_1 > 0$ and $c_2 > 0$ are constants which are related to the wing area of UAV, load factor and wing span efficiency etc., g is the gravitational acceleration, and m is the mass of the UAV including all its payload.

B. CHANNEL MODEL

In the satellite-to-UAV communication model, we suppose that the link between the satellite and UAV experiences widely-adopted Shadowed-Rician fading for practical purpose. In particular, the factors, such as the mobility feature of the UAV, have negligible effect on the changes of the distance and angle between the satellite and UAV, which are ignored in our model. Thus, the channel gain $h_{s,u}$ from the satellite to UAV can be respectively modeled as

$$h_{s,u} = \chi(\theta_u) \bar{h}_{s,u}, \quad (2)$$

with

$$\begin{cases} \chi(\theta) = \left(\frac{J_1(\lambda)}{2\lambda} + 36 \frac{J_3(\lambda)}{\lambda^3} \right)^2, \\ \lambda = 2.07123 \frac{\sin\theta}{\sin\theta_{3dB}}, \\ \bar{h}_{s,u} = A_u \exp(j\varphi_u) + Z_u \exp(j\psi_u), \end{cases}$$

where θ is the angle between the location of the corresponding receiver and the beam center with respect to the satellite,

and θ_{3dB} is the 3-dB angle. $\chi(\theta)$ is the corresponding beam gain factor, which is determined by their location. J_1 and J_3 represent the first-kind Bessel function of order 1 and 3, respectively. $\bar{h}_{s,u}$ denotes the channel fading from the satellite to UAV, which includes the scattering and the line-of-sight (LoS) components. φ_u denotes the stationary random phase with element uniformly distributed over $[0, 2\pi)$ and ψ_u denotes the deterministic phase of the LoS component. A_u and Z_u are the amplitudes of the scattering and the LoS components, respectively.

In the UAV-to-ground communication model, we suppose that the UAV/vehicle-mounted base station is equipped with a single antenna with omnidirectional unit gain. The UAV-to-vehicle channel model in suburban environments is adopted to only consider the effect of the environment on the occurrence of LoS, where the Doppler effect due to the relative mobility between UAV and ground vehicle is assumed to be compensated perfectly. Based on the above assumptions, the channel power gain at time slot n follows the free-space path loss model given by

$$h_{u,v}[n] = \frac{\mu_0}{\|\mathbf{w}[n] - \mathbf{l}_v[n]\|^2 + h^2}, \tag{3}$$

where $\mu_0 = (\frac{4\pi f_c}{c})^{-2}$ denotes the channel power gain at the reference distance of 1 meter, with f_c denoting the carrier frequency and c denoting the speed of light.

C. PROBLEM FORMULATION

In the considered satellite-air-ground integrated system, the UAV-mounted BS is assumed to operate in a full-duplex mode. The resulting self-interference can be perfectly cancelled by some existing self-interference cancellation techniques, such as absorptive shielding and cross-polarization. Simultaneously, the UAV-mounted BS adopts the amplify-and-forward strategy to achieve the goal of the small processing delay. In addition, the coordinated multi-point transmission is employed over the licensed frequency spectrum, and the satellite communication adopts the different frequency spectrum in the air-ground communication. Thus, the achievable rate of the ground vehicle $R_v[n]$ and the achievable rate of UAV $R_u[n]$ within time slot n can be respectively expressed as

$$\begin{cases} R_v[n] = \log_2(1 + \gamma_v[n]), \\ R_u[n] = \log_2(1 + \gamma_u[n]), \end{cases} \tag{4}$$

with

$$\begin{cases} \gamma_v[n] = \dfrac{p_u[n]h_{u,v}[n]p_s[n-1]h_{s,u} + p_b[n]h_{b,v}[n]}{p_u[n]h_{u,v}\sigma_u^2 + p_{b'}h_{b',v}[n] + \sigma_v^2}, \\ \gamma_u[n] = \dfrac{p_s[n]h_{s,u}}{\sigma_u^2}, \end{cases} \tag{5}$$

where $p_u[n]$ and $p_b[n]$ are respectively the transmission power of UAV and BS b_n within time slot n; p_s and $p_{b'}$ are respectively the transmission power of the satellite and BS b_n; $h_{b,v}[n]$ ($h_{b',v}[n]$) is the channel gain from BS b (BS b') to the vehicle within time slot n; σ_v^2 and σ_u^2 are respectively the power of the additive white Gaussian noise at the vehicle and the UAV.

The goal of this work is to maximize the sum-rate of the ground vehicle over the duration T by the joint optimization of power control as well as UAV's trajectory. Thus, the problem can be formulated as follows:

$$P1: \max_{\mathbf{w}[n],\mathbf{v}[n],\mathbf{a}[n],p_u[n],p_b[n]} \sum_{n=1}^{N} R_v[n] \tag{6a}$$

$$\text{s.t. } B_v R_v[n] \le B_u R_u[n-1], n = 1, 2, \ldots, N, \tag{6b}$$

$$\Xi(\mathbf{v}[n], \mathbf{a}[n]) < \frac{Q^{\max}}{\Delta t}, \tag{6c}$$

$$\mathbf{w}[n+1] = \mathbf{w}[n] + \mathbf{v}[n]\Delta t + \frac{\mathbf{a}[n]\Delta t^2}{2}, \quad n = 0, \ldots, N-1, \tag{6d}$$

$$\mathbf{v}[n+1] = \mathbf{v}[n] + \mathbf{a}[n]\Delta t, \quad n = 0, 1, \ldots, N-1, \tag{6e}$$

$$\mathbf{w}[0] = \mathbf{w}_0, \quad \mathbf{w}[N] = \mathbf{w}_F, \tag{6f}$$

$$\mathbf{v}[0] = \mathbf{v}_0, \quad \mathbf{v}[N] = \mathbf{v}_F, \tag{6g}$$

$$\|\mathbf{v}[n]\| \le v^{\max}, \quad n = 0, 1, \ldots, N, \tag{6h}$$

$$\|\mathbf{v}[n]\| \ge v^{\min}, \quad n = 0, 1, \ldots, N, \tag{6i}$$

$$\|\mathbf{a}[n]\| \le a^{\max}, \quad n = 0, 1, \ldots, N-1, \tag{6j}$$

$$0 \le p_u[n] \le p_u^{\max}, \quad n = 1, 2, \ldots, N, \tag{6k}$$

$$0 \le p_b[n] \le p_b^{\max}, \quad n = 1, 2, \ldots, N, \tag{6l}$$

where constraint (6b) is given to ensure that the UAV can receive sufficient data which is transmitted to the vehicle at any time slot n; B_u and B_v are the bandwidth of the satellite and the UAV, respectively; constraint (6c) is to guarantee that the stored energy of UAV can meet the consumption during the flight time T; (6d) and (6e) represent the velocity constraint and the acceleration constraint at the next time slot; (6f) denotes the UAV's initial location and final location constraint; (6g) denotes the UAV's initial velocity and final velocity constraint; (6h) and (6j) are the mobility constraints with the maximum UAV speed $v^{\max}$ and the maximum UAV acceleration $a^{\max}$; (6k) and (6l) represent the transmit power constraints of the UAV and the BS; $p_u^{\max}$ and $p_b^{\max}$ are respectively the peak power budget of the UAV and the BS.

IV. JOINT TRAJECTORY AND POWER OPTIMIZATION ALGORITHM

Since $P1$ is a joint optimization problem of the trajectory of UAV and power control, it is more complicated and also confronted with the significant challenge to solve the nonlinear problem. To address this intractable issue, we decompose $P1$ into two subproblems by optimizing two classes of variables alternately.

A. POWER OPTIMIZATION WITH FIXED TRAJECTORY

By fixing the UAV trajectory $\{\mathbf{w}[n], \mathbf{v}[n], \mathbf{a}[n]\}_{n=1}^N$, we first consider the following sub-problem $P2$ for optimizing the power allocations of the UAV and BS $\{p_u[n], p_b[n]\}_{n=1}^N$. Furthermore, since the link rate $R_v[n]$ monotonically

increases with SINR $\gamma_v[n]$, $P1$ with fixed trajectory thus reduces to

$$P2: \max_{p_u[n],p_b[n]} \sum_{n=1}^{N} R_v[n] \quad \text{s.t. (6b), (6k), (6l),} \tag{7}$$

It can be verified that the objective function is non-convex with respect to (w.r.t.) power control. We introduce the logarithmic approximation to convert $P2$ into a convex optimization problem.

Lemma 1: The objective function in $P2$ can be approximated to a concave form, that is $\sum_{n=1}^{N} R_v[n] \geq \sum_{n=1}^{N} \tilde{R}_v[n]$, which is given by (9). What's more, the equality between the left item and the right item in (9) is held when $p_u[n] = p_u^t[n]$.

Proof: To begin with, we define a function $g(x) = \ln(Ex + F)$ where E and F are negative constants. It can be trivially concluded that $g(x)$ is concave with respect to x. According to the fact that the value of the concave function is smaller than or equal to that of its first-order Taylor expansion at any point, we obtain the following inequation.

$$g(x) \leq \ln(Ex_0 + F) + \frac{E}{Ex_0 + F}(x - x_0), \tag{8}$$

where the equality is held when $x = x_0$.

By using this approximation method and letting $p_u^t[n]$ describe the transmit power of UAV in the t-th iteration, the objective function can be approximated to (9), as shown at the bottom of this page, where $A_n = p_s[n-1]h_{u,v}[n]h_{s,u}$, $B_n = h_{b,v}[n]$, $C_n = p_{b'}h_{b',v}[n] + \sigma_v^2$, and $D = h_{u,v}\sigma_u^2$.

Then, we get $\tilde{R}_v[n] = \frac{1}{\ln 2}\ln(1 + \frac{p_u[n]A_n + p_b[n]B_n}{C_n + p_u[n]D})$ if $p_u[n] = p_u^t[n]$. Namely, the equivalent condition between $R_v[n]$ and $\tilde{R}_v[n]$ is $p_u[n] = p_u^t[n]$.

In addition, the Hessian matrix of the function $\tilde{R}_v[n]$ for variables $p_u[n]$ and $p_b[n]$ can be expressed as

$$\nabla^2 \tilde{R}_v[n](p_u[n], p_b[n]) = \begin{bmatrix} \frac{-(A_n + D)^2}{H_n} & \frac{-(A_n + D)B_n}{H_n} \\ \frac{-(A_n + D)B_n}{H_n} & \frac{-B_n^2}{H_n} \end{bmatrix}, \tag{10}$$

where $H_n = (p_u[n](A_n + D) + p_b[n]B_n + C_n)^2$. It can be concluded that the Hessian matrix is negative semi-definite, and then $\tilde{R}_v[n]$ is concave w.r.t. $p_u[n]$ and $p_b[n]$ for $n \in \{1, 2, \ldots, N\}$.

Therefore, Lemma 1 is completed. ■

For constraint $B_v R_v[n] \leq B_u R_u[n-1]$ for $\forall n = 1, 2, \ldots, N$, the inequality is linear and rewritten as

$$p_u[n](A_n - DG_n) + p_b[n]B_n \leq C_n G_n, \tag{11}$$

where $G_n = 2^{\frac{B_u R_u[n-1]}{B_v}} - 1$.

When the approximate function proposed in Lemma 1 is used to replace the original objective function, we get the following problem.

$$P3: \max_{p_u[n],p_b[n]} \sum_{n=1}^{N} \tilde{R}_v[n] \quad \text{s.t. (11), (6k), (6l),} \tag{12}$$

According to Lemma 1, $P3$ is equivalent to $P2$ when $p_u[n] = p_u^t[n]$ for $\forall n = 1, 2, \ldots, N$, and also $P3$ is actually a convex problem, whose solution can be efficiently found via standard convex optimization tools, e.g., CVX. Nevertheless, we can analytically characterize the optimal solution to $P3$.

Theorem 1: The optimal solution to $P3$ is given by

$$\begin{cases} p_u^{\text{opt}}[n] = [p_u^t[n]]_0^{p_u^{\max}}, \\ p_b^{\text{opt}}[n] = [\frac{C_n G_n - p_u^t[n](A_n - DG_n)}{B_n}]_0^{p_b^{\max}}, \end{cases} \tag{13}$$

where $[z]_x^y \triangleq \min\{\max\{x, z\}, y\}$.

Proof: By introducing the Lagrange multipliers $\{\lambda_n\}_{n=1}^N$, the corresponding Lagrange function is given by (14).

$$\begin{aligned} &\mathcal{L}(p_u[n], p_b[n], \lambda_n) \\ &= \sum_{n=1}^{N} \tilde{R}_v[n] \\ &\quad + \sum_{n=1}^{N} \lambda_n \left(C_n G_n - p_u[n](A_n - DG_n) - p_b[n]B_n\right), \end{aligned} \tag{14}$$

Since $P3$ is a convex optimization problem, the optimal solutions need to satisfy the Karush-Kuhn-Tucker (KKT) conditions. Letting $\frac{\partial \mathcal{L}}{\partial p_u[n]} = 0$ and $\frac{\partial \mathcal{L}}{\partial p_b[n]} = 0$ for $\forall n = 1, 2, \ldots, N$, we have

$$\begin{aligned} \frac{\partial \mathcal{L}}{\partial p_u[n]} &= \frac{(A_n + D)}{\ln 2(p_u[n](A_n + D) + p_b[n]B_n + C_n)} \\ &\quad - \frac{D}{\ln 2(C_n + p_u^t[n]D)} - \lambda_n(A_n - DG_n) = 0, \end{aligned} \tag{15}$$

$$\begin{aligned} \frac{\partial \mathcal{L}}{\partial p_b[n]} &= \frac{B_n}{\ln 2(p_u[n](A_n + D) + p_b[n]B_n + C_n)} \\ &\quad - \lambda_n B_n = 0, \end{aligned} \tag{16}$$

$$\begin{aligned} R_v[n] &= \frac{1}{\ln 2}\left(\ln(p_u[n](A_n + D) + p_b[n]B_n + C_n) - \ln(C_n + p_u[n]D)\right) \\ &\geq \frac{1}{\ln 2}\left(\ln(p_u[n](A_n + D) + p_b[n]B_n + C_n) - \ln(C_n + p_u^t[n]D) - \frac{D}{C_n + p_u^t[n]D}(p_u[n] - p_u^t[n])\right) \\ &= \tilde{R}_v[n] \end{aligned} \tag{9}$$

and

$$\lambda_n \left(C_n G_n - p_u[n](A_n - DG_n) - p_b[n]B_n\right) = 0. \quad (17)$$

According to (15) and (16), the Lagrange multiplier λ_n is obtained by

$$\lambda_n = \frac{1}{\ln 2(C_n + p_u^t[n]D)(1 + G_n)}. \quad (18)$$

It follows from (18) that $\lambda_n \neq 0$. By submitting (17) into (15), we get

$$p_u[n] = p_u^t[n]. \quad (19)$$

Thus, from (17), we have

$$p_b[n] = \frac{C_n G_n - p_u^t[n](A_n - DG_n)}{B_n}. \quad (20)$$

■

B. UAV TRAJECTORY OPTIMIZATION WITH FIXED POWER

By fixing the power allocations of the satellite, the UAV and BS $\{p_u[n], p_b[n]\}_{n=1}^N$, we consider the following sub-problem $P4$ for optimizing the UAV trajectory $\{\mathbf{w}[n], \mathbf{v}[n], \mathbf{a}[n]\}_{n=1}^N$. Thus, $P1$ with fixed power reduces to

$$P4: \max_{\mathbf{w}[n],\mathbf{v}[n],\mathbf{a}[n]} \sum_{n=1}^{N} R_v[n]$$
$$\text{s.t. (6b), (6c), (6d), (6e), (6f), (6g), (6h), (6i), (6j).} \quad (21)$$

The problem $P4$ is intractable for the reason of the non-convex objective function and constraint (6c) w.r.t. the UAV trajectory. Thus, we use successive convex optimization technique to approximate $P4$ as a convex optimization problem.

For the objective function, it is not concave w.r.t. $\mathbf{w}[n]$, but is convex w.r.t. $\|\mathbf{w}[n] - \mathbf{l}_v[n]\|^2$. By first-order Taylor expansion at any local point, we can get the lower bound of $R_v[n]$. First, $R_v[n]$ can be rewritten as

$$R_v[n] = \log_2(1 + \frac{\Delta_1[n] + \Delta_2[n]\|\mathbf{w}[n] - \mathbf{l}_v[n]\|^2}{\Delta_3[n] + \Delta_4[n]\|\mathbf{w}[n] - \mathbf{l}_v[n]\|^2}), \quad (22)$$

where $\Delta_1[n] = p_u[n]\mu_0 p_s[n-1]h_{s,u} + p_b[n]h_{b,v}[n]h^2$, $\Delta_2[n] = p_b[n]h_{b,v}[n]$, $\Delta_3[n] = p_u[n]\mu_0\sigma_u^2 + (p_{b'}h_{b',v}[n] + \sigma_v^2)h^2$, and $\Delta_4[n] = p_{b'}h_{b',v}[n] + \sigma_v^2$.

Then, the lower bound to $R_v[n]$ with the given UAV's location $\mathbf{w}_t[n]$ in the t-th iteration can be deduced in (23), as shown at the bottom of this page. It is trivial to verify that $R_{v,t}[n]$ is a concave function w.r.t. $\mathbf{w}[n]$ when $\Delta_2[n]\Delta_3[n] - \Delta_1[n]\Delta_4[n] < 0$.

For constraint $B_v R_v[n] \leq B_u R_u[n-1]$ for $\forall n = 1, 2, \ldots, N$, the inequality can be rewritten as

$$\|\mathbf{w}[n] - \mathbf{l}_v[n]\|^2 \geq \frac{\Delta_1[n] - \Delta_3[n]G_n}{\Delta_4[n]G_n - \Delta_2[n]}. \quad (24)$$

with the constraint $\Delta_4[n]G_n - \Delta_2[n] > 0$. The left side of (24) is convex, and we can obtain a lower bound by the first-order Taylor expansion at the given local point $\mathbf{w}_t[n]$. Then, inequality (24) is converted to

$$\|\mathbf{w}_t[n] - \mathbf{l}_v[n]\|^2 + 2(\mathbf{w}_t[n] - \mathbf{l}_v[n])^T(\mathbf{w}[n] - \mathbf{w}_t[n]) \geq \frac{\Delta_1[n] - \Delta_3[n]G_n}{\Delta_4[n]G_n - \Delta_2[n]}. \quad (25)$$

To ensure that the above results hold, we give the following proposition.

Proposition 1: If the power optimization problem $P2$ is solved by Theorem 1, $\Delta_2[n]\Delta_3[n] - \Delta_1[n]\Delta_4[n] < 0$ and $\Delta_4[n]G_n - \Delta_2[n] > 0$ hold with $B_u > B_v$.

Proof: Let $F_1 = \Delta_2[n]\Delta_3[n] - \Delta_1[n]\Delta_4[n]$ and $F_2 = \Delta_4[n]G_n - \Delta_2[n]$. F_1 can be rewritten as

$$F_1 = -p_u[n]\mu_0(p_s[n-1]h_{s,u}p_{b'}h_{b',v}[n] - p_b[n]h_{b,v}[n]\sigma_u^2) - p_u[n]\mu_0 p_s[n-1]h_{s,u}\sigma_v^2. \quad (26)$$

To prevent that the signal from satellite is submerged with the back-ground noise in practice, the strength of the amplify-and-forward signal received by UAV-mounted relay needs to be much larger than noise strength. Since $p_s[n-1]p_{b'} - p_b[n] > 0$ and $h_{s,u}h_{b',v}[n] - h_{b,v}[n]\sigma_u^2 > 0$, we can deduce that $F_1 < 0$

For F_2, we have

$$F_2 = (p_{b'}h_{b',v}[n] + \sigma_v^2)G_n - p_b[n]h_{b,v}[n] \quad (27)$$

Since $\{p_b[n]\}_{n=1}^N$ is obtained by Theorem 1, (27) is converted to

$$F_2 = \begin{cases} (p_{b'}h_{b',v}[n] + \sigma_v^2)G_n - p_b^{\text{opt}}[n]h_{b,v}[n], p_b[n] \neq 0, \\ (p_{b'}h_{b',v}[n] + \sigma_v^2)G_n, p_b[n] = 0, \end{cases} \quad (28)$$

where $p_b^{\text{opt}}[n] = \min\{\frac{C_n G_n - p_u^t[n](A_n - DG_n)}{B_n}, p_b^{\max}\}$

(1) When $p_b[n] = 0$, $F_2 > 0$.

(2) When $p_b[n] = \frac{C_n G_n - p_u^t[n](A_n - DG_n)}{B_n}$, we have

$$F_2 = G_n\left(p_{b'}h_{b',v}[n] + \sigma_v^2 - \frac{(C_n - p_u^t[n](\frac{A_n}{G_n} - D))h_{b,v}[n]}{B_n}\right) = p_u^t[n]h_{u,v}[n](p_s[n-1]h_{s,u} - G_n\sigma_u^2) \quad (29)$$

$$R_v[n] \geq \log_2(1 + \frac{\Delta_1[n] + \Delta_2[n]\|\mathbf{w}_t[n] - \mathbf{l}_v[n]\|^2}{\Delta_3[n] + \Delta_4[n]\|\mathbf{w}_t[n] - \mathbf{l}_v[n]\|^2}) + \frac{(\Delta_2[n]\Delta_3[n] - \Delta_1[n]\Delta_4[n])(\|\mathbf{w}[n] - \mathbf{l}_v[n]\|^2 - \|\mathbf{w}_t[n] - \mathbf{l}_v[n]\|^2)}{\ln 2(\Delta_3[n] + \Delta_4[n]\|\mathbf{w}_t[n] - \mathbf{l}_v[n]\|^2)(\Delta_1[n] + \Delta_3[n] + (\Delta_2[n] + \Delta_4[n])\|\mathbf{w}_t[n] - \mathbf{l}_v[n]\|^2)} = R_{v,t}[n] \quad (23)$$

If $B_u > B_v$, $G_n = 2^{\frac{B_u R_u[n-1]}{B_v}} - 1 = (1 + \frac{p_s[n-1]h_{s,u}}{\sigma_u^2})^{\frac{B_u}{B_v}} - 1 < \frac{p_s[n-1]h_{s,u}}{\sigma_u^2}$. Thus, $F_2 > 0$.

(3) When $\frac{C_n G_n - p_u^t[n](A_n - DG_n)}{B_n} > p_b^{\max}$, $F_2 > 0$.

Therefore, Proposition 1 is completed. ■

For constraints (6c), the slack variable τ_n is defined to replace $\mathbf{v}[n]$, and then the function Ξ is recast as

$$\Xi(\mathbf{v}[n], \tau[n]) = \sum_{n=1}^{N} \left(c_1 \|\mathbf{v}[n]\|^3 + c_2 \tau[n] \right) + \frac{1}{2} m (\|\mathbf{v}[T]\|^2 - \|\mathbf{v}[0]\|^2) < \frac{Q^{\max}}{\Delta t}, \quad (30)$$

with constraints

$$\begin{cases} \frac{1}{\|\mathbf{v}[n]\|} \left(1 + \frac{\|\mathbf{a}[n]\|^2}{g^2} \right) \le \tau[n], & n \in \{0, 1, \ldots, N-1\}, \\ \tau[n] \le \frac{1}{v^{\min}} \left(1 + (\frac{a^{\max}}{g})^2 \right), & n \in \{0, 1, \ldots, N-1\}. \end{cases} \quad (31)$$

Similarly, we adopt the first-order Taylor expansion at the given local points $\mathbf{v}_t[n]$ and $\tau_t[n]$ to give

$$\begin{aligned} (\|\mathbf{v}[n]\| + \tau[n])^2 \ge\ & (\|\mathbf{v}_t[n]\| + \tau_t[n])^2 \\ & + 2(\|\mathbf{v}_t[n]\| + \tau_t[n]) \frac{\mathbf{v}_t[n]^T}{\|\mathbf{v}_t[n]\|} (\mathbf{v}[n] - \mathbf{v}_t[n]) \\ & + 2(\|\mathbf{v}_t[n]\| + \tau_t[n])(\tau[n] - \tau_t[n]) \\ =\ & \phi(\mathbf{v}[n], \tau[n]), \end{aligned} \quad (32)$$

which is a linear function w.r.t. $\mathbf{v}[n]$ and $\tau[n]$. Then, the constraints (31) can be approximated to

$$\begin{cases} 2 + \frac{2\|\mathbf{a}[n]\|^2}{g^2} + \|\mathbf{v}[n]\|^2 + \tau[n]^2 \le \phi(\mathbf{v}[n], \tau[n]), \\ \tau[n] \le \frac{1}{v^{\min}} \left(1 + (\frac{a^{\max}}{g})^2 \right), n \in \{0, 1, \ldots, N-1\}. \end{cases} \quad (33)$$

Thus, the problem $P4$ can be approximated as

$$P5: \max_{\mathbf{w}[n], \mathbf{v}[n], \mathbf{a}[n], \tau_n} \sum_{n=1}^{N} R_{v,t}[n]$$
$$\text{s.t. } (25), (30), (33), (6d), (6e), (6f), (6g), (6h), (6j). \quad (34)$$

It can be observed that the objective function in $P4$ is concave now, since $R_v[n]$ is concave w.r.t. $\mathbf{w}[n]$. Moreover, constraints in (34) are all concave w.r.t. $\mathbf{w}[n]$. Thus, $P5$ is a convex optimization problem which can be solved by CVX effectively.

C. JOINT TRAJECTORY AND POWER OPTIMIZATION

Based on the analysis above, the original optimization problem $P1$ can be optimized alternately by solving $P2$ and $P5$. Since the two sub-problems can be respectively solved by Algorithm 1 and Algorithm 2, we proposed the block coordinate descent method to solve problem $P1$, labeled as Algorithm 3. For the reasons of respectively applying gradient descent method and SCA to Algorithm 1 and Algorithm 2, it can be proven that the two algorithms are convergent by referring to the work in [40]. In the following, we prove that Algorithm 3 can converge to an optimal joint trajectory and power control solution by optimizing the two sub-problems alternately.

Let $\mathbf{z} = \{\mathbf{w}[n], \mathbf{v}[n], \mathbf{a}[n]\}$, $\mathbf{p} = \{p_s[n], p_u[n]\}$, $P = \sum_{n=1}^{N} R_v[n](\mathbf{z}, \mathbf{p})$. Thus, $P(\mathbf{z}(t), \mathbf{p}(t))$ is the objective function

Algorithm 1 Power Optimization Algorithm

1: **Initialization:** Set the initial time index $t = 0$. Initialize $\{p_u^0[n]\}_{n=1}^N$.
2: **Loop For** $t = 0, 1, 2, \cdots$,
Calculate $\{p_u^{\text{opt}}[n]\}_{n=1}^N$ and $\{p_b^{\text{opt}}[n]\}_{n=1}^N$ according to (13).
Let $t = t + 1$ and $p_u^t[n] = p_u^{\text{opt}}[n]$ for $n = 1, 2, \ldots, N$.
If it converges to the required accuracy, stop the algorithm.
3: **End loop**
4: **Output:** $p_u^{\text{opt}}[n]$ and $p_b^{\text{opt}}[n]$ for $n = 1, \ldots, N$.

Algorithm 2 UAV Trajectory Optimization Algorithm

1: **Initialization:** Set the initial index $t = 0$ and $\mathbf{w}_t[n], \mathbf{v}_t[n]$ for $\forall n = 1, \ldots, N$.
2: **Loop For** $t = 1, 2, \cdots$,
3: **Step 1:** Update the optimal UAV trajectory, denoted as $\{\mathbf{w}^{\text{opt}}[n], \mathbf{v}^{\text{opt}}[n], \mathbf{a}^{\text{opt}}[n], \tau^{\text{opt}}[n]\}_{n=1}^N$ by solving problem $P5$.
4: **Step 2:** Update the local points $\mathbf{w}_t[n] = \mathbf{w}^{\text{opt}}[n]$, $\mathbf{v}_t[n] = \mathbf{v}^{\text{opt}}[n]$ and $\tau_t[n] = \tau^{\text{opt}}[n]$ for $\forall n = 1, \ldots, N$.
$t = t + 1$.
If it converges to the required accuracy, stop the algorithm.
5: **End loop**
6: **Output:** The UAV trajectory $\{\mathbf{w}^{\text{opt}}[n], \mathbf{v}^{\text{opt}}[n], \mathbf{a}^{\text{opt}}[n]\}$ for $n = 1, \ldots, N$.

Algorithm 3 Joint Trajectory and Power Optimization Algorithm

1: **Initialization:** Set the initial index $t = 0$, the initial UAV trajectory $\{\mathbf{w}[n], \mathbf{v}[n], \mathbf{a}[n]\}_{n=1}^N$, and a small tolerance value $\epsilon > 0$.
2: **Loop For** $t = 1, 2, \cdots$,
3: **Step 1:** According to the fixed UAV trajectory, the optimal power allocations $\{p_u^{\text{opt}}[n], p_b^{\text{opt}}[n]\}_{n=1}^N$ are obtained by solving Algorithm 1.
4: **Step 2:** According to the fixed power allocations, the optimal UAV trajectory $\{\mathbf{w}^{\text{opt}}[n], \mathbf{v}^{\text{opt}}[n], \mathbf{a}^{\text{opt}}[n]\}_{n=1}^N$ is obtained by solving Algorithm 2.
$t = t + 1$.
If the fractional increase of the objective value of $P1$ is less than tolerance ϵ, stop the algorithm.
5: **End loop**
6: **Output:** The UAV trajectory $\{\mathbf{w}^{\text{opt}}[n], \mathbf{v}^{\text{opt}}[n], \mathbf{a}^{\text{opt}}[n]\}$ and the power allocations $\{p_u^{\text{opt}}[n], p_b^{\text{opt}}[n]\}$ for $t = 1, 2, \cdots, N$.

value in t-th iteration of Algorithm 3. Since the solution $\mathbf{p}(t+1)$ is obtained at step 1 of Algorithm 3 with given $\mathbf{z}(t)$, the following inequality holds: $P(\mathbf{z}, \mathbf{p}) \leq P(\mathbf{z}, \mathbf{p}(t+1))$. Similarly, the inequality $P(\mathbf{z}, \mathbf{p}(t+1)) \leq P(\mathbf{z}(t+1), \mathbf{p}(t+1))$ holds, where $\mathbf{z}(t+1)$ is obtained at step 2 of Algorithm 3 with given $\mathbf{p}(t+1)$. Then, we have $P(\mathbf{z}, \mathbf{p}) \leq P(\mathbf{z}(t+1), \mathbf{p}(t+1))$. It is obviously obtained that after each iteration, the objective value of problem $P1$ is monotonically non-decreasing and the objective value of $P1$ is upper bounded by a finite value. Thus, Algorithm 3 is guaranteed to converge.

V. SIMULATION RESULTS AND ANALYSIS

In this section, numerical simulations are performed by Matlab software to validate the efficiencies and performance of the proposed algorithm, which is used to solve the joint trajectory and power optimization problem for V2N communication in space-air-ground integrated green IoT networks

A. SIMULATION CONFIGURATION

In our simulations, we consider that a ground vehicle runs on the road from point (0, 0) to point (3000, 0) with a constant speed $v = 10$ m/s. The vehicle is served by the infrastructure, which consists of the roadside BSs and one UAV. The roadside BSs with altitude 30m are regularly deployed based on the interval of 1000 meters, and one UAV flies from (100, 100) to (3000, 100) with a fixed altitude $h = 200$m. The flight time of UAV is set to $T = 300$s and the duration of each time slot is $\Delta t = 5$s. For the UAV, the maximum transmit power $p_u^{\max}$, the maximum speed $v^{\max}$ and the maximum acceleration $a^{\max}$ are respectively set to 1W, 20m/s and 30m/s^2. The maximum transmit power of each BS is $p_b^{\max} = 10$W. The noise power at the vehicle is $\sigma_v^2 = -110$dBm.

Moreover, the UAV is connected to the content server by the satellite link. The distance between the satellite and UAV/vehicle is approximated to 3.6×10^7m. The transmit power of the satellite is $p_s[n] = 40$W. The noise power at the UAV is set to $\sigma_u^2 = -110$dBm. The beam angle from the satellite to vehicle is given as $\theta = 0.01°$. The channel fading distribution $h_{s,u}$ can be characterized as (ρ, ϱ, ϖ), with ρ being the average power of the LoS component, 2ϱ being the average power of the multi-path component, and ϖ being the Nakagami-m parameter corresponding to the fading severity. The corresponding parameters in the satellite link from the satellite to UAV with average shadowing is shown as $(\rho, \varrho, \varpi) = (0.835, 0.126, 10)$. Specifically, simulation parameters and values are listed in Table 1. Unless otherwise specified, there values are used in the sequel.

B. SIMULATION RESULTS AND ANALYSIS

To begin with, it is well known that the energy capacity of the battery-powered UAV exerts a strong impact on its flying trajectory. Fig. 2 plots the flying trajectories of UAV with different energy storage capacities. It is shown in Fig. 2 that UAV flies as close to the vehicle as possible to obtained a better channel condition if the UAV has stored enough energy. When the battery capacity is set to $Q^{\max} = 7.25 \times 10^5$J, it is shown that the UAV flies along a short path due to the lack of sufficient energy. Thus, an optimal trajectory planning is designed by Algorithm 3 on the strength of the enough energy storage.

TABLE 1. Simulation parameters.

Parameter	Value
Vehicle speed (v)	10 m/s
UAV flight time (T)	300 s
Length of time slot (Δt)	5 s
Vehicle initial/final position	(0,0), (3000,0)
UAV initial/final position	(100,100), (3000,100)
UAV altitude (h)	200 m
UAV maximum transmit power ($p_u^{\max}$)	1 W
Vehicle maximum speed ($v^{\max}$)	20 m/s
Vehicle maximum acceleration ($a^{\max}$)	30 m/s^2
BS maximum transmit power ($p_b^{\max}$)	10 W
Satellite transmit power ($p_s[n]$)	40 W
Beam angle (θ)	0.01°
Channel from satellite to UAV (ρ, ϱ, ϖ)	(0.835,0.126,10)
Distance between satellite and UAV/vehicle	3.6×10^7 m
Noise power (σ_v^2/σ_v^2)	-110 dBm

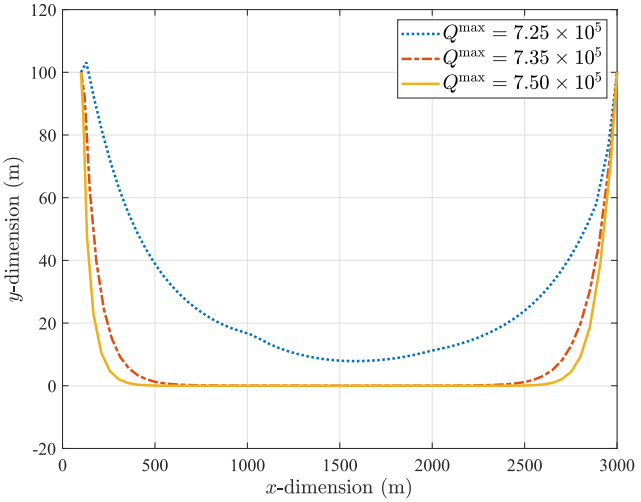

FIGURE 2. The trajectories of UAV with different energy storage capacities.

To further investigate the UAV trajectory under different driving strategies of the vehicle, we consider three schemes where the ground vehicle runs on the road from point (0, 0) to point (3000, 0) with uniform speed (labeled as case 1), two stages of acceleration and then uniform speed (labeled as case 2) or two stages of uniform speed and then deceleration (labeled as case 3). Letting the flight time T be set to 100s, Fig. 3 shows that the trajectories of UAV under three schemes. By comparing with Fig. 2, UAV under case 1 is inclined to forwardly move to the ending point in the latter stage due to the restriction of the flight time. In Fig. 3, UAV in case 2 flies from the starting point to the ending point according to U-shape trajectory where the the left inflexion point is closer to the vehicle compared with the right inflexion point. Since the vehicle in case 2 runs with first acceleration and then uniform speed, UAV has sufficient time to follow the vehicle with low speed at the beginning stage.

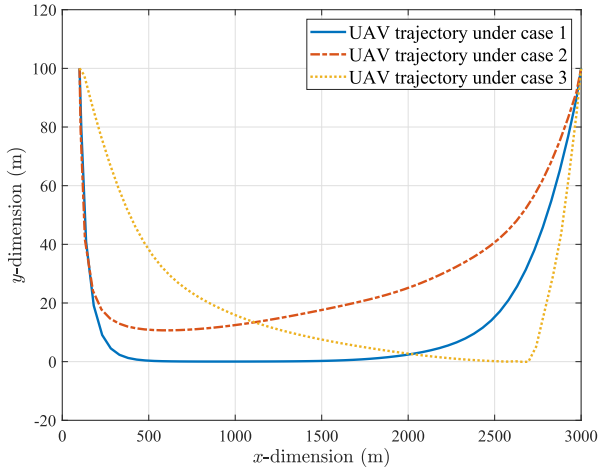

FIGURE 3. The trajectories of UAV under different vehicle speeds when the flight time T is set to 100s.

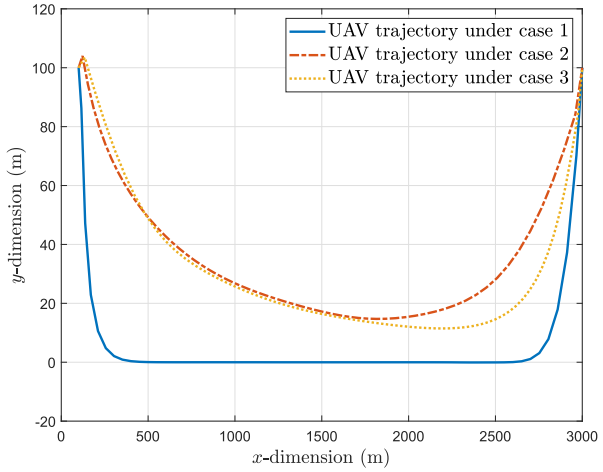

FIGURE 4. The trajectories of UAV under different vehicle speeds when the flight time T is set to 300s.

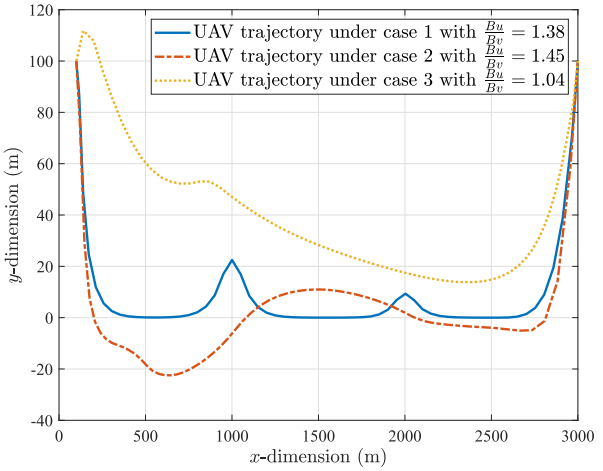

FIGURE 5. The trajectories of UAV under different vehicle speeds when the rate of bandwidth is set to different values.

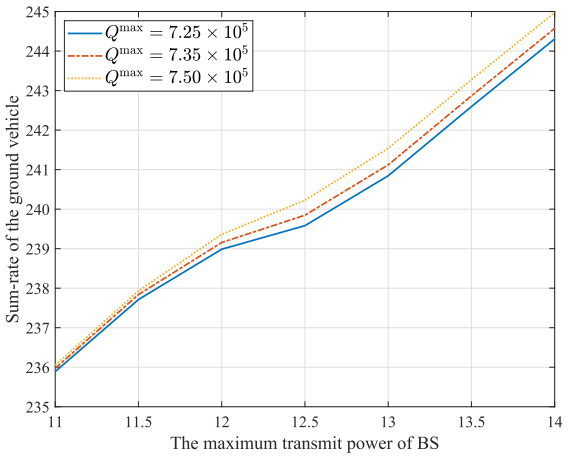

FIGURE 6. The sum-rate of the ground vehicle versus the maximum transmit power of BS with different energy storage capacities.

On the contrary, the right inflexion point of UAV trajectory in case 3 is closer to the vehicle. The main reason for this situation is the constraints of the whole flight time and the maximum flying speed. When the flight time T is set to 300s, Fig. 4 plots the trajectories of UAV under different vehicle speeds. Although the UAV has more time and desires to approach the vehicle, it is shown in Fig. 4 that other constraints play an negative role on the trajectory optimization of UAV when the vehicle speed is changed. Thus, the running speed of vehicle is one of factors influencing the UAV's trajectory (i.e., energy consumption).

In the following figure, we change the bandwidth rate between the satellite and UAV under three schemes, i.e. $\frac{B_u}{B_v} = 1.38$ in case 1, $\frac{B_u}{B_v} = 1.45$ in case 2 and $\frac{B_u}{B_v} = 1.04$ in case 3, and then plot the trajectory curves of UAV. By comparing with Fig. 3 and Fig. 4, it is shown in Fig. 5 that there are fluctuations on some time slots for UAV trajectories under three schemes if the bandwidth rate between the satellite and UAV is set to small value. Small bandwidth rate represents that UAV cannot receive more content from the satellite, and also it may result in the lack of enough data for UAV-relay transmission. For this reason, UAV has to fly away from the ground vehicle to obtain a worse channel state in some time slots. Therefore, a better flight strategy can be designed to improve communication quality and decrease energy consumption in line with green objective by altering the bandwidth rate.

Fig. 6 plots the curves of sum-rate of the ground vehicle as the maximum transmit power of BS increases under the different energy storage capacities of UAV. By comparison of the different battery capacities, i.e., setting $Q^{\max} = 7.25 \times 10^5$J, 7.35×10^5J or 7.50×10^5J, it is found that higher sum-rate is obtained if the battery capacity is expanded. This stems from the contribution of a better trajectory planning. It is noted from Fig. 6 that the gap on account of changing $Q^{\max}$ increases when the maximum transmit power of BS increases ranging from 11 to 13. The overall performance in the proposed communication model can be further improved by relaxing the power constraint of BS. It is also seen that the gap is small when the maximum transmit power of BS is set to 11. Thus, we can make a tradeoff

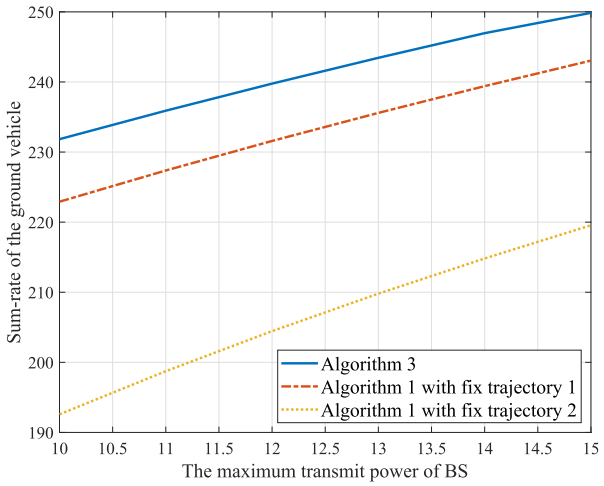

FIGURE 7. The sum-rate of the ground vehicle versus the maximum transmit power of BS with different UAV flying strategies.

between higher performance and green communication with less cost.

In order to verify the effectiveness of Algorithm 2, we give two predefined flight paths of UAV to compare with the proposed trajectory. The fixed trajectory 1 is that the UAV travels back and forth between the starting point (100,100) and ending point (3000,100) along the straight line at a uniform speed within the flight time T. The fixed trajectory 2 is that the UAV flies on the ellipse with two vertexes (1500,100) and (3000,0) at a uniform speed within the flight time T. Fig. 7 gives the performance comparison between joint optimizing power and trajectory and only optimizing power with fixed trajectory. It is shown in Fig. 7 that the sum-rate of the ground vehicle increases as the maximum transmit power of BS increases. Moreover, the sum-rate of the ground vehicle obtained by Algorithm 3 is obviously higher than that by the fixed trajectories, especially the fixed trajectory 2. By comparison, it is clearly seen that the UAV trajectory obtained by Algorithm 3 is longer than trajectory 1 and shorter than trajectory 2. It is known that the flying length is proportional to the carrying energy. Therefore, an optimal flight path for UAV can be achieved by using Algorithm 3 to save energy in line with green objective as well as ensure excellent communication performance with the vehicle.

VI. CONCLUSION

This paper investigated the space-air-ground integrated green IoT network, where the UAV with the help of the satellite as well as BS adopted the joint transmission method to enhance V2N communication performance. The goal of this paper was to maximize the vehicle's achievable rate by jointly optimizing the transmit power and UAV trajectory with UAV energy constraint and UAV mobility constraint. Then, we equivalently converted the optimization problem into two subproblems by fixing UAV trajectory or the power allocations. When the UAV trajectory was fixed, the optimal power allocations of UAV and BS were obtained by using the Lagrange method. On the other hand, the UAV trajectory under the fixed power allocations was obtained by using SCA method. Through the iterative alternation of two methods, the joint optimal solution maximizing the achievable rate was converged. Finally, numerical results verified that the vehicle can achieve a higher service performance under the condition of reducing the energy consumption of UAV by the UAV-aided wireless communication design.

REFERENCES

[1] B. Ahlgren, M. Hidell, and E. C.-H. Ngai, "Internet of Things for smart cities: Interoperability and open data," *IEEE Internet Comput.*, vol. 20, no. 6, pp. 52–56, Nov. 2016.

[2] J. Huang, Y. Meng, X. Gong, Y. Liu, and Q. Duan, "A novel deployment scheme for green Internet of Things," *IEEE Internet Things J.*, vol. 1, no. 2, pp. 196–205, Apr. 2014.

[3] J. Wu, M. Dong, K. Ota, J. Li, and W. Yang, "Application-aware consensus management for software-defined intelligent blockchain in IoT," *IEEE Netw.*, vol. 34, no. 1, pp. 69–75, Jan. 2020.

[4] J. Li, J. Wu, G. Xu, J. Li, X. Zheng, and A. Jolfaei, "Integrating NFV and ICN for advanced driver assistance systems," *IEEE Internet Things J.*, early access, Nov. 18, 2019, doi: 10.1109/JIOT.2019.2953988.

[5] T. Huang, W. Yang, J. Wu, J. Ma, X. Zhang, and D. Zhang, "A survey on green 6G network: Architecture and technologies," *IEEE Access*, vol. 7, pp. 175758–175768, 2019.

[6] H. Liang, J. Wu, S. Mumtaz, J. Li, X. Lin, and M. Wen, "MBID: Micro-blockchain-based geographical dynamic intrusion detection for V2X," *IEEE Commun. Mag.*, vol. 57, no. 10, pp. 77–83, Oct. 2019.

[7] V. Petrov, A. Samuylov, V. Begishev, D. Moltchanov, S. Andreev, K. Samouylov, and Y. Koucheryavy, "Vehicle-based relay assistance for opportunistic crowdsensing over narrowband IoT (NB-IoT)," *IEEE Internet Things J.*, vol. 5, no. 5, pp. 3710–3723, Oct. 2018.

[8] Z. Wan, Z. Pan, W. Ni, F. Wang, Z. Qiu, S. Liu, and Z. Xu, "A vehicle mobile Internet of Things coverage enhancement algorithm based on communication duration probability analysis," *IEEE Access*, vol. 7, pp. 98356–98365, 2019.

[9] L. Liang, G. Y. Li, and W. Xu, "Resource allocation for D2D-enabled vehicular communications," *IEEE Trans. Commun.*, vol. 65, no. 7, pp. 3186–3197, Jul. 2017.

[10] J. Wu, M. Dong, K. Ota, J. Li, and Z. Guan, "FCSS: Fog-computing-based content-aware filtering for security services in information-centric social networks," *IEEE Trans. Emerg. Topics Comput.*, vol. 7, no. 4, pp. 553–564, Oct. 2019.

[11] J. Wu, M. Dong, K. Ota, J. Li, W. Yang, and M. Wang, "Fog-computing-enabled cognitive network function virtualization for an information-centric future Internet," *IEEE Commun. Mag.*, vol. 57, no. 7, pp. 48–54, Jul. 2019.

[12] J. Wu, K. Ota, M. Dong, and C. Li, "A hierarchical security framework for defending against sophisticated attacks on wireless sensor networks in smart cities," *IEEE Access*, vol. 4, pp. 416–424, 2016.

[13] J. Wu, M. Dong, K. Ota, J. Li, and Z. Guan, "Big data analysis-based secure cluster management for optimized control plane in software-defined networks," *IEEE Trans. Netw. Service Manage.*, vol. 15, no. 1, pp. 27–38, Mar. 2018.

[14] J. Chen, G. Mao, C. Li, W. Liang, and D.-G. Zhang, "Capacity of cooperative vehicular networks with infrastructure support: Multiuser case," *IEEE Trans. Veh. Technol.*, vol. 67, no. 2, pp. 1546–1560, Feb. 2018.

[15] M. Zheng, S. Chen, W. Liang, and M. Song, "NSAC: A novel clustering protocol in cognitive radio sensor networks for Internet of Things," *IEEE Internet Things J.*, vol. 6, no. 3, pp. 5864–5865, Jun. 2019.

[16] H. Lu, X. He, M. Du, X. Ruan, Y. Sun, and K. Wang, "Edge QoE: Computation offloading with deep reinforcement learning for Internet of Things," *IEEE Internet Things J.*, early access, Mar. 17, 2020, doi: 10.1109/JIOT.2020.2981557.

[17] C. Tang, L. Song, J. Balasubramani, S. Wu, S. Biaz, Q. Yang, and H. Wang, "Comparative investigation on CSMA/CA-based opportunistic random access for Internet of Things," *IEEE Internet Things J.*, vol. 1, no. 2, pp. 171–179, Apr. 2014.

[18] C. Guo, L. Liang, and G. Y. Li, "Resource allocation for low-latency vehicular communications: An effective capacity perspective," *IEEE J. Sel. Areas Commun.*, vol. 37, no. 4, pp. 905–917, Apr. 2019.

[19] Z. Chang, S. Zhou, T. Ristaniemi, and Z. Niu, "Collaborative mobile clouds: An energy efficient paradigm for content sharing," *IEEE Wireless Commun.*, vol. 25, no. 2, pp. 186–192, Apr. 2018.

[20] Z. Zhou, J. Feng, C. Zhang, Z. Chang, Y. Zhang, and K. M. S. Huq, "SAGECELL: Software-defined space-air-ground integrated moving cells," *IEEE Commun. Mag.*, vol. 56, no. 8, pp. 92–99, Aug. 2018.

[21] W. Feng, J. Wang, Y. Chen, X. Wang, N. Ge, and J. Lu, "UAV-aided MIMO communications for 5G Internet of Things," *IEEE Internet Things J.*, vol. 6, no. 2, pp. 1731–1740, Apr. 2019.

[22] N. H. Motlagh, T. Taleb, and O. Arouk, "Low-altitude unmanned aerial vehicles-based Internet of Things services: Comprehensive survey and future perspectives," *IEEE Internet Things J.*, vol. 3, no. 6, pp. 899–922, Dec. 2016.

[23] K. An, M. Lin, J. Ouyang, and W.-P. Zhu, "Secure transmission in cognitive satellite terrestrial networks," *IEEE J. Sel. Areas Commun.*, vol. 34, no. 11, pp. 3025–3037, Nov. 2016.

[24] H. Dai, Y. Huang, J. Wang, and L. Yang, "Resource optimization in heterogeneous cloud radio access networks," *IEEE Commun. Lett.*, vol. 22, no. 3, pp. 494–497, Mar. 2018.

[25] N. Kato, Z. M. Fadlullah, F. Tang, B. Mao, S. Tani, A. Okamura, and J. Liu, "Optimizing space-air-ground integrated networks by artificial intelligence," *IEEE Wireless Commun.*, vol. 26, no. 4, pp. 140–147, Aug. 2019.

[26] J. Liu, Y. Shi, Z. M. Fadlullah, and N. Kato, "Space-air-ground integrated network: A survey," *IEEE Commun. Surveys Tuts.*, vol. 20, no. 4, pp. 2714–2741, 4th Quart., 2018.

[27] J. Mei, K. Zheng, L. Zhao, Y. Teng, and X. Wang, "A latency and reliability guaranteed resource allocation scheme for LTE V2V communication systems," *IEEE Trans. Wireless Commun.*, vol. 17, no. 6, pp. 3850–3860, Jun. 2018.

[28] H. Ye, G. Y. Li, and B. F. Juang, "Deep reinforcement learning based resource allocation for V2V communications," *IEEE Trans. Veh. Technol.*, vol. 68, no. 4, pp. 3163–3173, Apr. 2019.

[29] D. Xu, P. Ren, and J. A. Ritcey, "Reliability and accessibility of low-latency V2I channel training protocol using cover-free coding: Win–win or tradeoff?" *IEEE Trans. Veh. Technol.*, vol. 68, no. 3, pp. 2294–2305, Mar. 2019.

[30] L. Liang, S. Xie, G. Y. Li, Z. Ding, and X. Yu, "Graph-based resource sharing in vehicular communication," *IEEE Trans. Wireless Commun.*, vol. 17, no. 7, pp. 4579–4592, Jul. 2018.

[31] Y. Wang, K. Venugopal, A. F. Molisch, and R. W. Heath, "MmWave vehicle-to-infrastructure communication: Analysis of urban microcellular networks," *IEEE Trans. Veh. Technol.*, vol. 67, no. 8, pp. 7086–7100, Aug. 2018.

[32] M. Jia, X. Zhang, X. Gu, and Q. Guo, "Energy efficient cognitive spectrum sharing scheme based on inter-cell fairness for integrated satellite-terrestrial communication systems," in *Proc. IEEE 87th Veh. Technol. Conf. (VTC Spring)*, Jun. 2018, pp. 1–6.

[33] B. Li, Z. Fei, X. Xu, and Z. Chu, "Resource allocations for secure cognitive satellite-terrestrial networks," *IEEE Wireless Commun. Lett.*, vol. 7, no. 1, pp. 78–81, Feb. 2018.

[34] Z. Lin, M. Lin, J.-B. Wang, Y. Huang, and W.-P. Zhu, "Robust secure beamforming for 5G cellular networks coexisting with satellite networks," *IEEE J. Sel. Areas Commun.*, vol. 36, no. 4, pp. 932–945, Apr. 2018.

[35] Y. Zhang, X. Zhu, C. Jiang, and L. Yin, "Joint user access and resource association in multicast terrestrial-satellite cooperation network," in *Proc. IEEE Globecom Workshops (GC Wkshps)*, Dec. 2018, pp. 1–6.

[36] S. H. Chae, C. Jeong, and K. Lee, "Cooperative communication for cognitive satellite networks," *IEEE Trans. Commun.*, vol. 66, no. 11, pp. 5140–5154, Nov. 2018.

[37] M. Hua, Y. Wang, M. Lin, C. Li, Y. Huang, and L. Yang, "Joint CoMP transmission for UAV-aided cognitive satellite terrestrial networks," *IEEE Access*, vol. 7, pp. 14959–14968, Jan. 2019.

[38] L. Ruan, J. Wang, J. Chen, Y. Xu, Y. Yang, H. Jiang, Y. Zhang, and Y. Xu, "Energy-efficient multi-UAV coverage deployment in UAV networks: A game-theoretic framework," *China Commun.*, vol. 15, no. 10, pp. 194–209, Oct. 2018.

[39] C. Joo and J. Choi, "Low-delay broadband satellite communications with high-altitude unmanned aerial vehicles," *J. Commun. Netw.*, vol. 20, no. 1, pp. 102–108, Feb. 2018.

[40] H. Dai, Y. Wang, T. Zhou, and L. Yang, "Joint service improvement and content placement for cache-enabled heterogeneous cellular networks," *IET Signal Process.*, vol. 13, no. 3, pp. 253–261, May 2019.

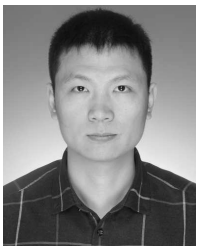

HAIBO DAI (Member, IEEE) received the M.S. degree from Yanshan University, Qinhuangdao, China, in 2013, and the Ph.D. degree in electrical engineering from Southeast University, Nanjing, China, in 2017. Since February 2018, he has been a Faculty Member with the School of the Internet of Things, Nanjing University of Posts and Telecommunications. His current research interests include wireless resource allocation and management, vehicle-to-everything communications, unmanned aerial vehicle communications, optimization in space-air-ground integrated networks, game theory, and artificial intelligence in 5G networks and beyond. He has published many articles in international journals, such as the IEEE JOURNAL ON SELECTED AREAS IN COMMUNICATIONS and the IEEE TRANSACTIONS ON VEHICULAR TECHNOLOGY, as well as articles in conferences, such as the IEEE Wireless Communications and Networking Conference and the IEEE Global Communications Conference.

HUI BIAN received the B.S. degree from the School of Information Science and Engineering, Southeast University, Nanjing, China, in 2016, where she is currently pursuing the M.S. degree in information systems and communications. Her research interests focus on energy-efficient wireless communication, UAV communications, and optimization techniques.

CHUNGUO LI (Senior Member, IEEE) received the bachelor's degree in wireless communications from Shandong University, in 2005, and the Ph.D. degree in wireless communications from Southeast University, Nanjing, China, in 2010. In July 2010, he joined the Faculty of Southeast University, where he became an Associate Professor, in 2012, an Advisor of the Ph.D. degree students, in 2016, and a Full Professor, in 2017. From June 2012 to June 2013, he was the Postdoctoral Researcher with Concordia University, Montreal, QC, Canada. From July 2013 to August 2014, he was with the DSL Laboratory, Stanford University, as a Visiting Associate Professor. From August 2017 to July 2019, he was an Adjunct Professor with Xizang Minzu University, under the supporting Tibet program organized by China National Human Resources Ministry. His research interests are in wireless communications and cyberspace security, and machine learning-based image/video signal processing.

BAOYUN WANG (Member, IEEE) received the Ph.D. degree in electrical engineering from Southeast University, Nanjing, China, in 1997. He was a Postdoctoral Research Fellow with the Department of Computer Science and Engineering, Pohang University of Science and Technology, Pohang, South Korea, from 1999 to 2000, with the Department of Electronic Engineering, City University of Hong Kong, from 2000 to 2002, with the Department of Mathematics and Computer Science, University of Sydney, from 2004 to 2005. He is currently a Full Professor in electrical engineering with the Nanjing University of Posts and Telecommunications, Nanjing. His research interests include the area of statistical signal processing, information theory, and their applications in wireless communications.